25 June 1999

ELSEVIER

Chemical Physics Letters 307 (1999) 95–101

CHEMICAL PHYSICS LETTERS

Theoretical study of solvent and temperature effects on the behaviour of poly(ethylene oxide) (PEO)

Beatriz A. Ferreira [a], Hélio F. Dos Santos [a,b], Américo T. Bernardes [c], Glaura G. Silva [d], Wagner B. De Almeida [a,*]

[a] *Laboratório de Química Computacional e Modelagem Molecular, Departamento de Química, ICEx, UFMG, Belo Horizonte, MG, 31270-901, Brazil*

[b] *Departamento de Química, ICE, UFJF, Juiz de Fora, MG, 36036-330, Brazil*

[c] *Departamento de Física, ICEB, UFOP, Ouro Preto, MG, 35400-00, Brazil*

[d] *Laboratório de Materiais, Departamento de Química, ICEx, UFMG, Belo Horizonte, MG, 31270-901, Brazil*

Received 27 May 1998; in final form 15 April 1999

Abstract

Molecular mechanics and molecular dynamics simulations were applied in order to study the behaviour of poly(ethylene oxide) (PEO) in different temperatures and solvents. It was found that over the temperature range of 50–500 K the equilibrium structure of PEO is folded. Both kinetic and potential energies increase with temperature. The behaviour of PEO in two different solvents – $CHCl_3$ ($\varepsilon = 5$) and H_2O ($\varepsilon = 80$) – was found to be similar, with the folded structure observed in equilibrium. The solvation energy calculated using the GB/SA model yielded essentially the same value in $CHCl_3$ and H_2O.

1. Introduction

Computational simulation techniques are powerful tools for learning about local structures and dynamics in various types of systems. Conformational studies of biological macromolecules have been carried out in order to understand peptide bonds, stability and protein folding [1,2].

Poly(ethylene oxide) (PEO) of low molecular weight, in the range 200–20 000, is used in cosmetics, lubricants, pharmaceuticals, electronics and other applications [3]. These polymeric systems derived from ethylene oxide exhibit low toxicity, good stability and lubricity. They can also be mixed with water or other solvents to give a wide range of viscosities. The presence of the electron-rich oxygen atoms in the backbone structure of the polymers offers a site for coordination and the ability of electron-poor groups to associate with these polymers is important for their use in many applications. PEO has been proposed to be an important polymer in drug release systems [4] and for dissolving salts in electrolyte complexes [5–7].

As mentioned before, the presence of an oxygen atom in every third position produces special physical–chemical properties, for example solubility, crystallinity and flexibility and complexation power, which are often very different from those of the

* Corresponding author. E-mail: wagner@netuno.qui.ufmg.br

0009-2614/99/$ - see front matter
PII: S0009-2614(99)00501-1

parent compound. In this Letter molecular mechanics and dynamics simulation studies were carried out in order to investigate the structural and energetic behaviour of PEO containing 20 monomeric units in different temperatures and solvents. This work intends to be a contribution to the study of the special properties of this polymer that are of increasingly fundamental and technological interest.

2. Methodology

Molecular simulations are based on empirical force fields, which describe interatomic interactions and mechanical deformation of molecules. The classical equations of Newton (motion equations) are numerically integrated using empirical force fields for all atoms of the system and the total energy is assumed to be dependent on both bond lengths and angles as well as non-bonded interactions and torsion angle terms (Coulomb and van der Waals interactions).

The molecular dynamics study of PEO containing 20 monomeric units was performed using the OPLS (optimised potentials for liquid simulations) force field [8] implemented in the Macromodel program [9]. The approximated energy of a molecular structure or a set of molecules is calculated from the molecular mechanics energy terms whose equations describe stretching, bending, torsion, van der Waals and electrostatic energies, as described elsewhere [10], using the EPROX routine of Macromodel [9].

The GB/SA (generalised born surface area) model [11] was used to include the solvent effect in the system. This model considers solvation free energy (G_{sol}) as consisting of a solvent–solvent cavity term (G_{cav}), a solute van der Waals term (G_{vdW}) and a solute–solvent electrostatic polarisation term (G_{pol}):

$$G_{sol} = G_{cav} + G_{vdW} + G_{pol}\,. \qquad (1)$$

G_{sol} for saturated hydrocarbons in water is linearly related to the solvent-accessible surface area (SA) and is evaluated by setting

$$G_{cav} + G_{vdW} = \sum \sigma_k \mathrm{SA}_k\,, \qquad (2)$$

where SA_k is the total solvent accessible surface area of atoms of type k, and σ_k is an empirical atomic solvation parameter.

The G_{pol} expression has been termed the generalised Born (GB) equation and could be described by the simple following equation:

$$G_{pol} = -166\left(1 - \frac{1}{\varepsilon}\right)\sum_{i=1}^{n}\sum_{j=1}^{n}\frac{q_i q_j}{f_{GB}}\,, \qquad (3)$$

where $f_{GB} = (r_{ij}^2 + \alpha_{ij}^2 e^{-D})^{1/2}$ is defined by the r_{ij} distance between i and j, $\alpha_{ij} = (\alpha_i \alpha_j)^{1/2}$ (in which α_i and α_j are the Born radii of i and j, respectively, and $D = r_{ij}^2/(2\alpha_{ij})^2$); q_i, q_j = atomic charges; and ε = dielectric constant [11].

The calculated solvation energy has two contributions, termed solvation energies 1 ($G_{cav} + G_{vdW}$) and 2 (G_{pol}).

In the temperature-dependent MDM study, two structures were used as initial configurations. For the temperatures $T = 50$, 90, 100, 150, 280, 298, 333 and 500 K a minimised linear structure was used. At lower temperatures ($T = 50$, 90, 100 and 150 K) the simulations were also started with an initial folded structure (the equilibrium conformation obtained at $T = 298$ K). For $T = 150$ K, we started the simulation with another folded structure which corresponded to the minimum potential energy in the $T = 50$ K simulation (at $t = 419$ ps). As a special case, a simulation with decreasing temperature was carried out over the range 300–50 K. The system was simulated in a vacuum during $t = 1\,000$ ps and the time step was $\Delta t = 1$ fs.

The entropic contribution for the folding process was analysed using the semiempirical method AM1 (Austin Model I) [12]. The calculations were performed at 100, 298 and 500 K, using the last structures obtained from the MD simulations. The linear and folded geometries were fully optimised at the semiempirical level and the thermodynamics properties were calculated at the different temperatures using the statistical thermodynamics formalism.

The behaviour of PEO as function of solvent was also studied. The inclusion of solvent was accomplished by using the GB/SA model, previously described. Simulations were performed at a fixed temperature (298 K) using a minimised linear structure as the initial point. The system was simulated in a vacuum ($\varepsilon = 1$), $CHCl_3$ ($\varepsilon = 5$) and H_2O ($\varepsilon = 80$) with a time step equal to $\Delta t = 1$ fs during a total time of $t = 1\,000$ ps.

3. Results and discussions

Fig. 1 shows the equilibrium structures obtained after 1 000 ps of simulation in the temperature range of 50–500 K. Depending on the initial configuration (linear or folded), we obtained different results for some simulations at low temperatures. We did not observe a polymer folding after 1 000 ps of simulation when the initial configuration was a minimised initial linear structure. However, by starting the simulations with a folded structure we observed that they remained folded indefinitely. As we will discuss

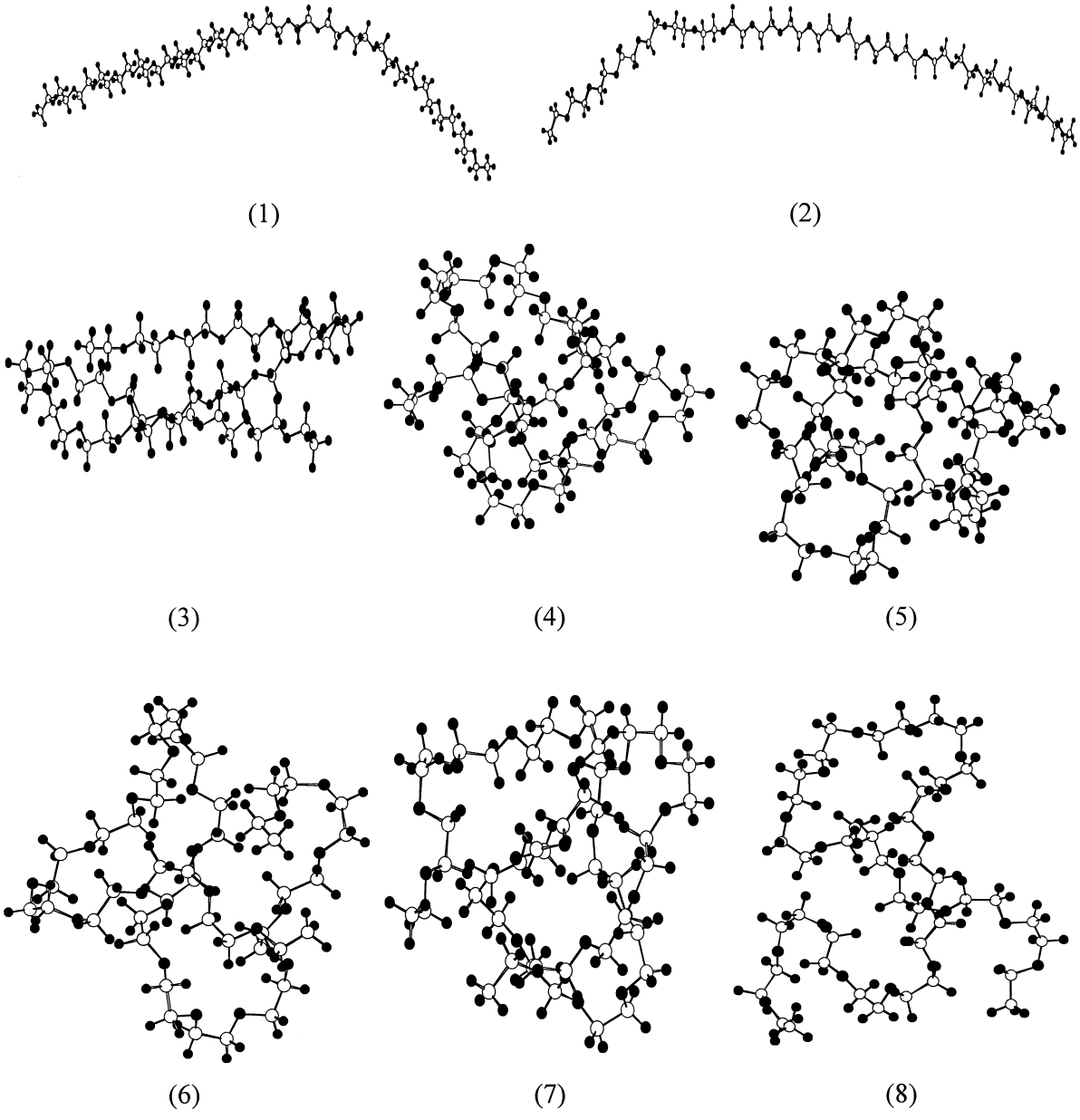

Fig. 1. Equilibrium structures for PEO at $T = 50$ (1), 90 (2), 100 (3), 150 (4), 280 (5), 298 (6), 333 (7) and 500 K (8). Initial configurations were all a linear minimised structure.

below, we have always obtained folded structures as the equilibrium ones for all temperatures. At lower temperatures, one cannot fold the initial linear structure. The rigidity observed in this case is due to the low probability of occurrence of torsion, which allows the molecule to fold, which means that the potential barrier is too high. Therefore, only for very long time simulations ($t \to \infty$) could significant changes in the linear conformation be observed. Thus, we defined a linear final state as a meta-stable one. This analysis is confirmed by the fact that the conformational energy for a final folded structure after 1 000 ps of simulation is lower than that value for the folded initial structure. We used as the initial configuration that final folded structure obtained for $T = 298$ K. When different simulations were done and different final configurations have been obtained, we choose as equilibrium configurations those which present – on average – a lower potential energy. Fig. 2 shows an example of how the system reaches the equilibrium state. We plotted the potential energy vs. time for three different simulations: starting with a linear structure (crosses), with a folded structure obtained for $T = 298$ K (open triangles) and with the minimum potential energy folded structure obtained for $T = 50$ K (filled circles). As one can observe, the potential energy of the equilibrium fluctuates around 290 kJ/mol and only after $t \approx 900$ ps has the structure represented by crosses

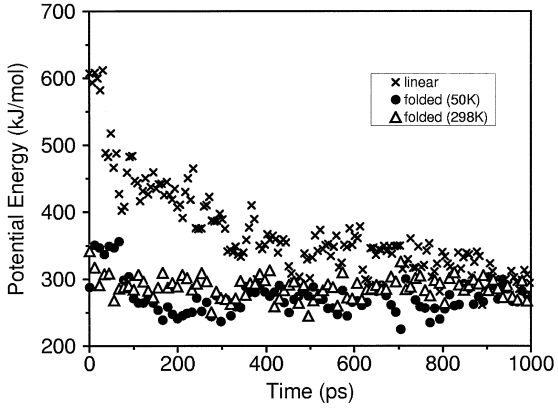

Fig. 2. Potential energy vs. time for simulations at $T = 150$ K. Three initial configurations were used: (1) a linear structure; (2) a folded structure obtained as a final structure for simulation at $T = 298$ K; and (3) the folded structure with lowest potential energy for simulations at $T = 50$ K.

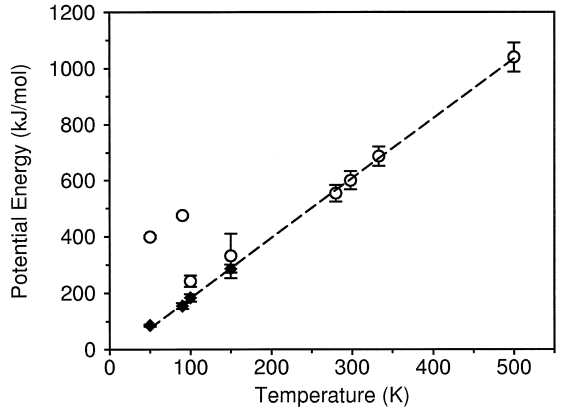

Fig. 3. Potential energy vs. temperature. The values of the potential energy of the initial configurations were discarded (typically $t < 300$ ps) in order to get equilibrium values. Open circles represent the values obtained for simulations which started with linear structures. Filled diamonds started with folded structures. The equilibrium values show a linear dependence on the temperature.

reached that value. The other two values fluctuate around the equilibrium energy, although that represented by filled circles shows more fluctuations. We assume that this occurs due to the fact that the initial configuration (for $T = 50$ K) is more folded than that expected for $T = 150$ K. So, the unfolding process presumably produces those fluctuations.

The increase of total average energy of the system is due to both kinetic and potential terms. Fig. 3 shows the values of the potential energy for all simulations. Open circles represent the simulation that started with a linear structure, while filled diamonds represent those which started with a folded structure. As one can observe, for lower temperatures (50, 90, 100, 150 K) the value of the potential energy is higher than that obtained for folded initial structure. Note that we used the data for the calculations which were obtained after the system reached the equilibrium, i.e., where the energy fluctuates around a stable value. Typically, we discarded the initial 300 ps of simulations. The small error bars obtained for the lowest temperatures (50, 90 and 100 K) come from the fact that they are in a meta-stable state – as discussed above – and that the fluctuations in this case are small. Note that for $T = 150$ K the potential energy (for the case where the initial structure was a linear one) has larger error bars, represent-

ing the fact that the system has not stabilised. The dashed line in this figure represents a linear regression made with the equilibrium values. Thus, we can assume that the equilibrium potential energy shows a linear dependence with the temperature for the complete temperature interval of our simulations.

Table 1 shows the fitting of the end-to-end carbon distances to Gaussian functions, using the data obtained from equilibrium structures. We observe an increase of the width of the peak at half height (Γ) and in the centre values (r) with increasing temperature. We related the end-to-end carbon distance (less folded structures) and increasing conformational distribution for PEO with the temperature increase. For higher temperatures, the width of the curve is of the order of the magnitude of its centre, while for lower temperatures this relation is around 30%. This means that for higher temperatures strong fluctuations are present.

In order to describe in more detail the equilibrium structures obtained in our simulations, we calculated the radius of gyration of the molecule for different temperatures. The radius of gyration R_g is given by

$$R_g = \sqrt{\frac{\sum m_i R_i^2}{\sum m_i}}\ , \qquad (4)$$

where m_i is the mass of the ith atom of the polymer, $\boldsymbol{R}_i = |\boldsymbol{r}_i - \boldsymbol{r}_{cm}|$, $\boldsymbol{r}_i$ is the actual position of the ith atom and $\boldsymbol{r}_{cm}$ is the centre of mass position of the polymer. Fig. 4 shows the results obtained for the equilibrium configurations. As one can observe, the higher the temperature is, the larger is the radius of gyration (the increase of the radius of gyration is not linear with temperature). Moreover, the fluctuations increase with temperature, the same phenomenon as observed for the end-to-end carbon distances. An interesting aspect that can be observed in Fig. 4 is the behaviour of the radius of gyration when a simulation is made by decreasing the temperature, where it is found that R_g decreases and remains

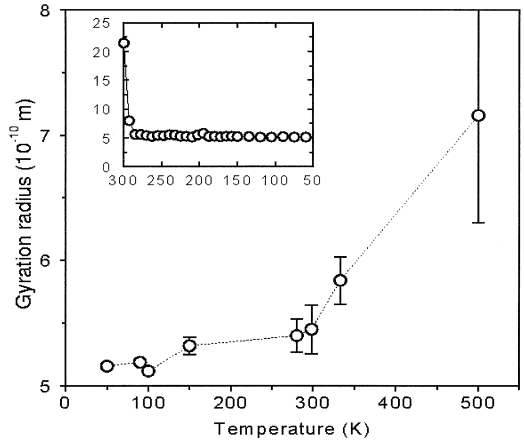

Fig. 4. Gyration radii of final configurations vs. temperature. The average was obtained taking into account the configurations at $t = 500$, 600, 700, 800, 900 and 1000 ps. The data show a non-linear dependence with temperature. The inset figure shows the gyration radii behaviour when the temperature is decreased in the MD simulation.

Table 1
Gaussian fitted parameters related to conformational population distribution curves as a function of end-to-end carbon distances over the temperature range 50–500 K

Temperature (K)	Centre, r (Å)	Width of the peak at half height, Γ (Å)
50	5.2	0.5
90	5.4	1.0
100	7.2	0.8
150	7.5	2.1
280	7.0	4.8
298	7.5	10.7
333	12.0	9.5
500	14.9	11.4

Table 2
Thermodynamic properties (in kcal/mol) for the folding process in the PEO molecule

T (K)	$\Delta H_T^{o\,a}$	$\Delta S_T^{o\,b}$	ΔZPE^c	$\Delta G_T^{o\,d}$
100[e]	−21.094	0.020	4.221	−18.873
100[f]	−23.158	0.022	5.860	−19.498
298	−17.284	0.051	5.929	−26.553
500	−5.979	0.080	5.717	−40.262

[a] $\Delta H_T^o = \Delta H_{f,T}^o(\text{folded}) - \Delta H_{f,T}^o(\text{linear})$, where the $\Delta H_{f,T}^o$ is the heat of formation calculated at the temperature T.
[b] $\Delta S_T^o = S_T^o(\text{folded}) - S_T^o(\text{linear})$.
[c] ΔZPE = ZPE(folded) − ZPE(linear). ZPE is the zero-point energy.
[d] $\Delta G_T^o = \Delta H_T^o - T\Delta S_T^o + \Delta$ZPE.
[e] Structure obtained from the simulation started with linear geometry.
[f] Structure obtained from the simulation started with folded geometry.

Table 3
Values of conformational energy terms (E in kJ/mol) for PEO containing 20 monomeric units in a vacuum, $CHCl_3$ and H_2O at 298 K

	Energy	E_{vacuum} (kJ/mol)	E_{CHCl_3} (kJ/mol)	E_{H_2O} (kJ/mol)
	kinetic	546	546	546
H	stretching	191	190	193
	bending	296	294	291
	torsion	118	120	111
	vdW	−103	−63	−101
	electrostatic	109	119	151
	$G_{vdW} + G_{cav}$	0	−118	64
	G_{pol}	0	−19	−171
	total energy[a]	1157	1067	1084

[a] Standard deviation ~ 2%.

practically constant. This means that folded structures are definitely preferable to linear ones.

In the discussion presented previously, only the enthalpic contribution to the free energy has been considered for the folding process analysis. In order to analyse the entropy (S^o) change, the semiempirical AM1 method [12] was used to calculate the S_T^o values for the linear and folded structures at $T = 100$, 298 and 500 K. The folded equilibrium structures obtained from the MD simulations at the respective temperatures were used as starting points in the geometry optimisation procedure at the semiempirical level. The fully optimised geometries were used in the calculation of the thermodynamic properties. The results obtained are reported in Table 2. Analysing the values in Table 2, an increase of ΔH^o with T, can be seen showing that the folding process should be less favourable at higher temperature when only the energetic contribution to the free energy is considered. However, when the entropic contribution (ΔS^o) is considered, the folding process was found to be more favourable (more negative values of ΔG^o) as the temperature rises, the term $-T\Delta S^o$ being dominant at $T > 298$ K.

Table 3 presents different contributions of the energetic terms obtained after simulations of the PEO in a vacuum, $CHCl_3$ and H_2O. By analysing the intramolecular potential, it was noted that the principal changes due to the solvent were observed for the van der Waals (vdW) and electrostatic interaction terms. Intermolecular contributions to the solvation process are present as ($G_{vdW} + G_{cav}$) and G_{pol}. The results of the calculations for ($G_{vdW} + G_{cav}$) showed an associated nature of the water because it needs an energy consumption to form cavities in the solvent. The G_{pol} term represents a solute–solvent electrostatic interaction energy, proportional to the dielectric constant of the medium. Fig. 5 shows the conformational population distribution as a function of end-to-end carbon distance. The end-to-end carbon distance (adjusted as described above) shows an

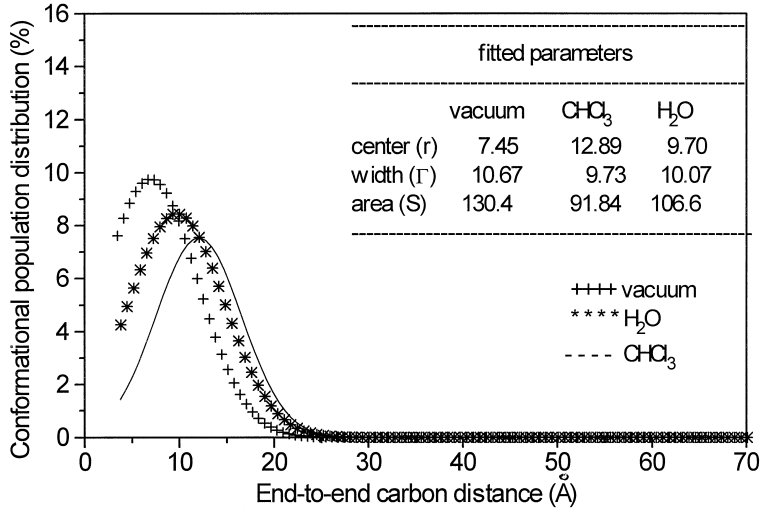

Fig. 5. Conformational population distribution as function of end-to-end carbon distance in vacuum, $CHCl_3$ and H_2O.

average distance increase as a function of the medium in the following order: $CHCl_3 > H_2O >$ vacuum. The structural effect described by the end-to-end carbon distance can be related to the degree of folding of the structure, considering that the principal energetic contribution in the macromolecules folding processes involves non-bonded atom interactions. The values obtained for the vdW terms can be used to justify the degree of folding observed in different media. These values showed that E_{vdW} has higher values (more repulsive) for $CHCl_3$ leading to less folded structures ($E_{vdW} = -63$ kJ/mol and $r = 12.89$ Å). It can be seen that $E_{vdW} = -103$ kJ/mol in the absence of solvent and $E_{vdW} = -101$ kJ/mol in H_2O carrying to more folded structures, in agreement with the centre distribution values shown in Fig. 5 ($r = 7.45$ Å in a vacuum and $r = 9.70$ Å in H_2O).

4. Conclusions

Mechanical and dynamic methods were applied in order to investigate the behaviour of PEO containing 20 monomeric units as a function of temperature and solvent. From the simulations performed in the temperature range of 50–500 K, we concluded that both kinetic and potential terms are responsible for the increase in the total energy as a function of temperature. We have obtained folded final structures as the equilibrium structures for all temperatures. For lower temperatures, the system might be 'trapped' in a meta-stable state when the simulations were started with a linear structure. Besides, we could relate the end-to-end carbon distance (less folded structures) and conformational distribution variation for PEO with an increase in temperature. Moreover, we also observed that the radius of gyration increases with temperature, but it did not show a linear dependence on the temperature. It was also observed that the entropic contribution is important for the folding process at higher temperature, the term $|-T\Delta S^o|$ being $> |\Delta H^o|$ at $T > 298$ K.

It was found that the behaviour of PEO in a vacuum, $CHCl_3$ and H_2O is similar, where a tendency of PEO to assume a folded structure in the equilibrium was shown. The solvation energy results, obtained using the GB/SA model, confirm this tendency. The values in both solvents ($CHCl_3$ and H_2O) were found to be close and slightly less than in a vacuum. The structural effect observed in the analysis of the end-to-end carbon distance equilibrium structures (average distance $CHCl_3 > H_2O >$ vacuum) was related to the non-bonded atom interactions.

Acknowledgements

The authors would like to thank the Conselho Nacional de Desenvolvimento Científico (CNPq) for providing the research grants. Thanks are also due to the Fundaçao de Amparo a Pesquisa do Estado de Minas Gerais (FAPEMIG) and the Programa de Apoio ao Desenvolvimento Científico e Tecnológico (PADCT, Proc. No. 62.0241/95.0) for supporting this project. HFDS would like to thank the Núcleo de Acesso Remoto-UFJF, CENAPAD-MG/CO, for the computational facilities.

References

[1] V.N.R. Pillai, M. Mutter, Acc. Chem. Res. 14 (1981) 122.
[2] A.D. Robertson, K.P. Murphy, Chem. Rev. 97 (1997) 1251.
[3] N. Clinton, P. Matlock, Encyclopedia of Polymers, Vol. 6, John Wiley & Sons, New York, 1986, p. 225.
[4] A. Apicela, B. Cappello, M.A. Del Nobile, M.I. La Rotonda, G. Mensitieri, L. Nicolais and S. Seccia, Polymeric Drugs and Drug Administration, Am. Chem. Soc., Washington, DC, 1994.
[5] M. Armand, Solid State Ionics 69 (1994) 309.
[6] K. Murata, Electrochim. Acta 40 (13) (1995) 2177.
[7] M. Armand, J.Y. Sanchez, M. Gauthier, Y. Choquette, in: J. Lipkowski, P.N. Ross (Eds.), Electrochemistry of Novel Materials, ch. 2, VCH, New York, 1994.
[8] W.L. Jorgensen, J. Tirado-Rives, J. Am. Chem. Soc. 110 (1988) 1657.
[9] F. Mohamadi, N.G.J. Richards, W.C. Guida, R. Liskamp, M. Lipton, C. Caufield, G. Chang, T. Hendrickson, W.C. Still, J. Comput. Chem. 11 (1990) 440.
[10] Special issue on Molecular Mechanics and Modelling, Chem. Rev. 93 (1993).
[11] W.C. Still, A. Tempczyk, R.C. Hawley, T. Hendrickson, J. Am. Chem. Soc. 112 (1990) 6127.
[12] M.J.S. Dewar, E.G. Zoebish, E.F. Healy, J.J.P. Stewart, J. Am. Chem. Soc. 107 (1985) 3902.